

LETTER

Open Access



Polyacetylenes and sesquiterpenes in Chinese traditional herb *Atractylodes lancea*: biomarkers and synergistic effects in red secretory cavities

Daiquan Jiang^{1,5,6†}, Huaibin Lin^{1†}, Zhenhua Liu^{2†}, Keke Qi^{3†}, Wenjin Zhang⁴, Hongyang Wang^{1,5}, Chengcai Zhang^{1,5}, Lu Zhu², Jiaojiao Zhu², Yan Zhang^{1,5}, Luqi Huang^{1,5}, Sheng Wang^{1,5*} , Yang Pan^{3*} and Lanping Guo^{1,5*}

The *Atractylodes lancea* rhizome (AR) stands as a significant source of traditional medicine in East Asia, widely recognized for its therapeutic properties in Traditional Chinese Medicine (TCM) (Chen et al. 2016; Zhang et al. 2021). These include liver protection, blood sugar control, diuretic effects, and anti-hypoxic activities, all attributed to its rich content of sesquiterpenoids (such as hinesol

and atractylon) and other medicinal components. These compounds have been shown to have anti-bacterial, anti-tumour, and blood sugar-lowering effects, with some, such as hinesol, demonstrating promise against lung cancer (Qin et al., 2019; Acharya et al. 2021a, b; Zhang et al. 2021). The quality of AR varies by region, with the Maoshan variety from Jiangsu, China (JAR), exhibiting the highest medicinal efficacy. The presence of red secretory cavities has long been considered a marker of high quality (Xu et al. 2022; Zhang et al., 2023). However, the specific cause of the colour variation remains unknown.

To investigate the marker metabolites within the distinct-colour secretory cavities (SCs) of AR, we conducted GC-MS analysis to discern the chemical composition variations among the red secretory cavities (RSCs), yellow secretory cavities (YSCs), and non-secretory cavities (NSCs) in JAR (Fig. 1a). Red secretory cavities (RSCs) contained the highest number of metabolites (74), while non-secretory cavities (NSCs) had the lowest (40) (Table S1, Fig S1a, b). Principal component analysis and heatmap clustering confirmed these results. Sesquiterpenes were the most abundant metabolites, with higher levels in RSCs. Further analysis identified unique metabolite compositions among red, yellow, and non-secretory cavities. Nine compounds were shared between red and yellow cavities, potentially contributing to the red coloration (Fig. 1b, S1c-f).

[†]Daiquan Jiang, Huaibin Lin, Zhenhua Liu and Keke Qi contributed equally to this work.

*Correspondence:

Sheng Wang

mmcnui@163.com

Yang Pan

panyang@ustc.edu.cn

Lanping Guo

glp01@126.com

¹ State Key Laboratory for Quality Assurance and Sustainable Use of Dao-di Herbs, National Resource Center for Chinese Materia Medica, China, Academy of Chinese Medical Sciences, Beijing 100700, PR China

² Joint Center for Single Cell Biology, Shanghai Collaborative Innovation Center of Agri-Seeds, School of Agriculture and Biology, Shanghai Jiao Tong University, Shanghai 200240, China

³ National Synchrotron Radiation Laboratory, University of Science and Technology of China, Hefei 230029, China

⁴ College of Pharmacy, Ningxia Medical University, Yinchuan 750004, China

⁵ Key Laboratory of Biology and Cultivation of Herb Medicine, Ministry of Agriculture and Rural Affairs, Beijing 100700, PR China

⁶ Agriculture and Biotechnology Center, South China, National Botanical Garden, Chinese Academy of Sciences, Guangzhou 510645, China



© The Author(s) 2025. **Open Access** This article is licensed under a Creative Commons Attribution 4.0 International License, which permits use, sharing, adaptation, distribution and reproduction in any medium or format, as long as you give appropriate credit to the original author(s) and the source, provide a link to the Creative Commons licence, and indicate if changes were made. The images or other third party material in this article are included in the article's Creative Commons licence, unless indicated otherwise in a credit line to the material. If material is not included in the article's Creative Commons licence and your intended use is not permitted by statutory regulation or exceeds the permitted use, you will need to obtain permission directly from the copyright holder. To view a copy of this licence, visit <http://creativecommons.org/licenses/by/4.0/>. The Creative Commons Public Domain Dedication waiver (<http://creativecommons.org/publicdomain/zero/1.0/>) applies to the data made available in this article, unless otherwise stated in a credit line to the data.

To enable a comprehensive comparison of metabolites across different AR samples, we meticulously selected three representative accessions (specifically JAR, HAR, SAR) exhibiting distinct cavity types from various geographic regions of China (Fig. 1c, S2). To enhance the resolution of chemical distribution in AR, we employed Laser Capture Microdissection (LCM) to isolate the SCs from micro-sections of AR from the three distinct *A. lancea* accessions. The SCs were further categorized by tissue type, encompassing the cortex, phloem, xylem, and pith (Fig. 1c). SCs contained more chemicals (56) than non-cavity areas (6) (Table S2, Fig. S3). SCs from accessions in different regions (HAR, JAR, SAR) had unique metabolic fingerprints. Orthogonal Partial Least Squares Discriminant Analysis (OPLS-DA) was used to identify metabolites that differed between red and non-red SCs (Fig. S4). The analysis showed a clear separation between the different comparison groups, suggesting unique metabolites in red SCs. Three specific polyacetylenes were consistently found in red compared to non-red SCs, and not in comparisons between different types of red SCs (Fig. 1d). This suggests that these three compounds are strongly associated with the red colour of the SCs. Further targeted analysis confirmed the presence of two of these polyacetylenes (atractylodin and (4*E*,6*E*,12*E*)-tetradecatriene-8,10-diyne-1,3-diol-diacetate) in red SCs (Fig. S5).

Utilizing the two identified datasets of differential metabolites from the secretory and non-secretory compartments of AR (Fig. 1b, d), we conducted a quantitative analysis on two common polyacetylenes (Fig. 1e). These included atractylodin (272.72 $\mu\text{g}/\mu\text{L}$ and 72.34 $\mu\text{g}/\mu\text{L}$ in YSC and RSC, respectively) and (4*E*,6*E*,12*E*)-tetradecatriene-8,10-diyne-1,3-diol-diacetate (58 $\mu\text{g}/\mu\text{L}$ and

7 $\mu\text{g}/\mu\text{L}$ in YSC and RSC, respectively). By simulating the actual concentrations within the secretory cavities using corresponding standard substances, the experiment confirmed that both metabolites are responsible for the red coloration in the SCs (Fig. 1f, g). The accumulation of differences in their concentrations directly caused the observed colour differences (red and yellow). This illustrates that the variation in the surface colour of AR is primarily attributed to differences in polyacetylene content. Furthermore, we collected SCs after LCM, extracted metabolites with 80% methanol, and analysed by LC-MS which is commonly used for analysing polar compounds. In total, 43 compounds were detected. Multivariate data analysis revealed no correlation between polar metabolites and red SCs (Table S3, Fig. S6). Altogether, our data indicated that the three non-polar polyacetylenes are the likely causal compounds related to the red SCs in *A. lancea* natural accessions.

We subsequently investigated whether the two polyacetylenes, atractylodin and (4*E*,6*E*,12*E*)-tetradecatriene-8,10-diyne-1,3-diol-diacetate, exhibited high *in situ* accumulation within the red SCs. Focusing on samples from JAR, which harbours two distinct SC types, particularly the cortex SCs with red secretory cavities, we used DESI/PI-MSI for spatial visualization of the major differential metabolites in frozen sections of JAR. Both atractylodin (*m/z* 183.0807) and (4*E*,6*E*,12*E*)-tetradecatriene-8,10-diyne-1,3-diol-diacetate (*m/z* 301.2164) revealed a strong correlation with the coloured SCs in JAR (Fig. 1h). The DESI/PI-MSI result for other polyacetylenes and sesquiterpenes are presented in Fig. S7. In conclusion, our results demonstrate that the high accumulation of atractylodin and (4*E*,6*E*,12*E*)-tetradecatriene-8,10-diyne-1,3-diol-diacetate is likely responsible for the cinnabar-coloured spots in AR.

(See figure on next page.)

Fig. 1 Biomarkers of red secretory cavities and the synergistic effect of polyacetylenes and sesquiterpenes in *Atractylodes lancea*. **a** Overview of sample acquisition and workflow. Red secretory cavities (RSC), yellow secretory cavities (YSC), and non-secretory cavities (NSC) samples were obtained from JAR with three independent biological repeats each. **b** Venn diagram depicting differential metabolites associated with red secretory cavities, highlighting shared and unique compounds among RSC, YSC, and NSC. **c** Overview of sample acquisition and workflow. Samples of AR from three different geographical origins, including transverse sections from Jiangsu (JAR), Shaanxi (SAR), and Hubei (HAR). Secretory cavities in cortex (Co-SC), phloem (Ph-SC), xylem (Xy-SC), and pith (Pi-SC) are indicated. **d** Venn diagram showing the three differential metabolites associated with the red secretory cavities. **e** Venn diagram illustrating the differential metabolites shared between differential metabolite set 1 (9 metabolites presented in Fig. 1b) and set 2 (3 metabolites presented in Fig. 1d). **f, g** Structural formulas of atractylodin (**f**) and (4*E*,6*E*,12*E*)-tetradecatriene-8,10-diyne-1,3-diol-diacetate (**g**), and their content differences among RSC, YSC, and NSC (mean \pm sem, $n=3$, *t*-test, $***P < 0.001$). Dissolving standard substances were used to simulate the colour differences of atractylodin and (4*E*,6*E*,12*E*)-tetradecatriene-8,10-diyne-1,3-diol-diacetate at different concentrations (concentration reference in quantitative results in **f** and **g**), solvent ethyl acetate). Bars = 1 cm. **h** The optical images of rhizome cross sections of JAR (selected trapezoid patch is marked with red dash line). And corresponding DESI/PI-MSI of selected ions (*m/z*). MS images were recorded with a scanning step size of 200 μm . Bar = 3 mm. **i** Effects of different ratios of essential oil components on the levels of TNF- α , IL-6, and IL-1 β in mouse colonic tissue (mean \pm sem, $n=8$). Stars indicate significant differences to the model group (*t*-test, $P < 0.05$). The experimental group Exp+All mirrors the compound composition found in JAR from the geographic region of Geo-herb, featuring 44% atractylon, 37% atractylodin, 8% hinesol, and 11% β -eudesmol. In contrast, Exp-Atd excludes atractylodin, while Exp-Atl omits atractylon. Exp-Hnl eliminates hinesol from the mixture, and Exp-Bem removes β -eudesmol.

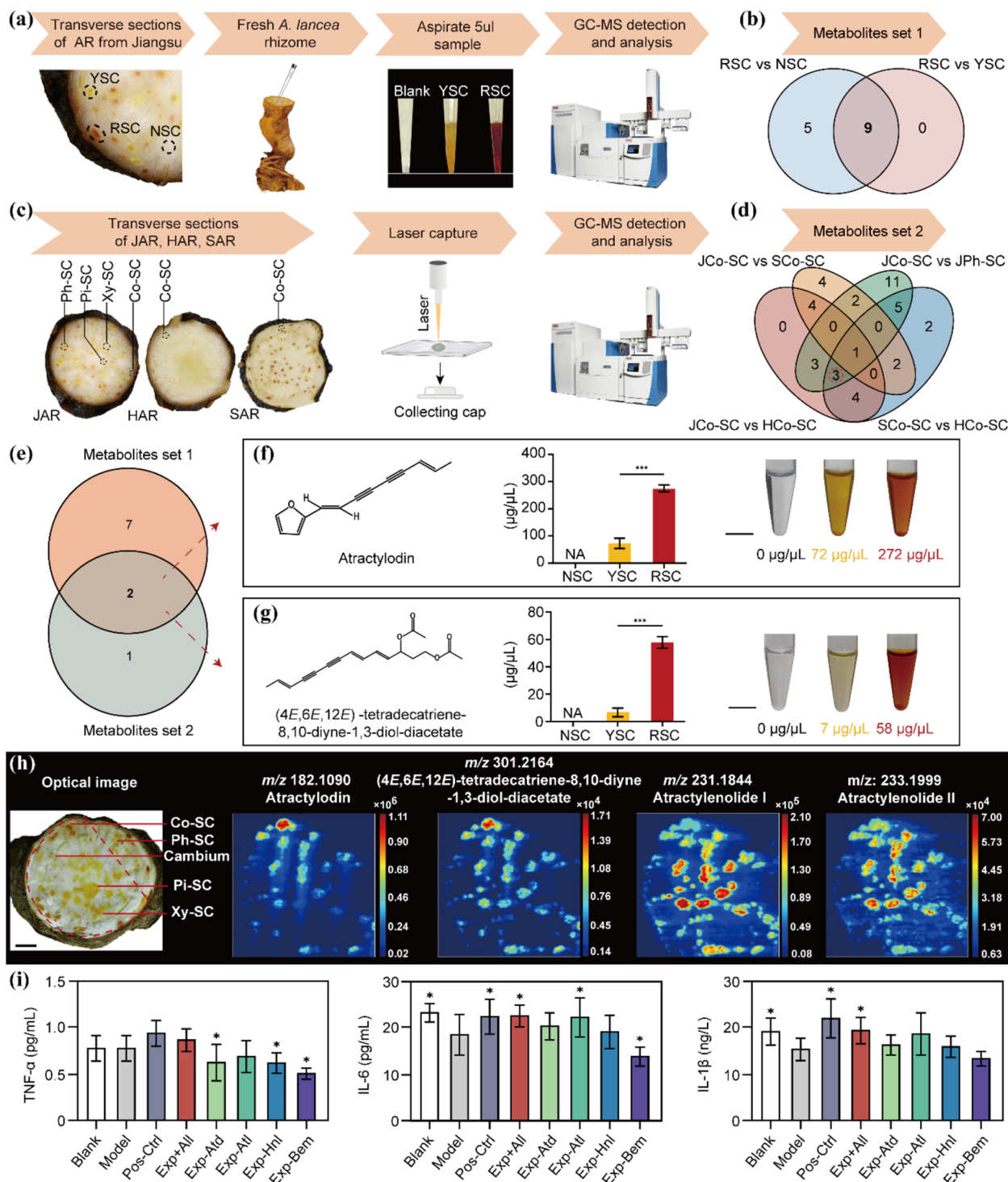


Fig. 1 (See legend on previous page.)

To date, several bioactive metabolites have been identified in AR, including atractylodin, atractylon, hinesol, and β -eudesmol (Zhang et al. 2021; Chen et al. 2023). In this study, we specifically identified atractylodin as a

biomarker for the red secretory cavities. This raises the question of whether the primary medicinal effect of AR is mainly attributed to atractylodin itself or to a synergistic interaction between atractylodin and other compounds.

To explore the impact of the key active components of *A. lancea* on digestive disorders, we utilized an ICR mouse model and treated them with different active compounds from AR in specific proportions (Table S4).

After a successful modelling period, mice in the experimental groups with different ratios of *A. lancea* essential oil demonstrated improvements in mental status, glossy fur, increased food intake, and enhanced activity, along with well-formed faeces (Fig. S8a, b). The body weight of mice in all groups gradually increased, with the most notable effects observed in experimental groups Exp+All and Exp-Atd. Additionally, the faecal moisture content of mice in each group exhibited a gradual increase, with a significant improvement in groups Exp+All and Exp-Bem compared to the modelling group (Fig. S8c).

Following the final administration, we assessed the serum levels of MTL, GAS, and VIP (Fig. S8d-f). Additionally, we measured three pro-inflammatory cytokines commonly associated with spleen deficiency: IL-1 β , IL-6, and TNF- α (Fig. 1i). Compared to the blank control group, the model group exhibited significantly increased serum levels of MTL, GAS, and VIP, accompanied by decreased levels of IL-6 and IL-1 β . Compared to the model group, GAS levels were restored in groups Exp-Atd, Exp-Atl, and Exp-Bem, while VIP levels were restored in most treatment groups except for group Exp-Atl. Notably, the treatment resembling JAR from the geographic region of Geo-herb (group Exp+All) significantly rescued both IL-6 and IL-1 β . Furthermore, we assessed the pathological changes in the colon using Haematoxylin and Eosin (HE) staining. Mice in experimental group Exp+All showed the most noticeable improvement in the arrangement and structural integrity of glandular and goblet cells within the colonic lumen (Fig. S8g). Collectively, our findings indicate that the optimal ratio of bioactive compounds, resembling that found in Geo-herbs, determines the best medicinal effect.

In summary, we systematically analysed two representative *A. lancea* natural accessions, each characterized by distinct secretory cavities. The results revealed two polyacetylenes, atractylodin and (4*E*,6*E*,12*E*)-tetradecatriene-8,10-diyne-1,3-diol-diacetate, that were significantly associated with the distinctive red coloration of secretory cavities in *A. lancea*. Although we employed various metabolomic methods, we acknowledge that there may be other important metabolites responsible for the coloration and medicinal efficacy due to the limitations of these methods and the complexity of TCM samples. Using a mouse model of diarrhoea induced by spleen deficiency, we further investigated whether the medicinal efficacy of AR is primarily attributed to atractylodin alone or to a synergistic interaction with other compounds. The results indicated that the authentic

chemical composition of *A. lancea* significantly ameliorates symptoms of spleen deficiency-induced diarrhoea in mice, with atractylodin playing a substantial role in the therapeutic effect. Our findings provide unprecedented insights into the molecular basis underlying the most optimal phenotype (cinnabar-like red secretory cavities) and the Geo-herbalism in TCM.

Supplementary Information

The online version contains supplementary material available at <https://doi.org/10.1186/s43897-024-00130-2>.

Supplementary Material 1

Supplementary Material 2.

Supplementary Material 3

Acknowledgements

We would like to express our sincere gratitude to Professor Xiang Zengxu from Nanjing Agricultural University for his invaluable assistance in collecting samples from Jiangsu Province (JAR), and to Professor Liu Dahui from Hubei University of Chinese Medicine for his support in gathering samples from Hubei Province (HAR).

Authors' contributions

S.W., L.G. & Y.P. conceived and designed the study; D.J., C.Z. L.H. & H.W. conducted sample preparation; D.J. & L.H. conducted laser capture microdissection, GC-MS and LC-MS analysis; K.Q. conducted DESI/PI-MSI measurements; W.Z. conduct pharmacological experiments; D.J., Z.L., L.H., W.Z., L.Z., J.Z., L.Z., Y.Z., S.W., L.G. & Y.P. analysed data; L.H. made some constructive suggestions for the manuscript. Z.L., D.J., K.Q., S.W., L.G. & Y.P. wrote the manuscript with input from all authors.

Funding

L.G. and S.W.' lab was financially supported by National Key Research and Development Program of China(2023YFC3503801); National Natural Science Foundation of China (No: 81891014); Scientific and technological innovation project of China Academy of Chinese Medical Sciences (CI2021A03903, CI2024C001YN, CI2023E002); Z.L.'s program was funded by a joint research funding (SA1500259) between Shanghai Jiao Tong University and University of Nottingham and Key Project at Central Government level: the ability establishment of sustainable use for valuable Chinese medicine resources (2060302).

Data availability

All datasets generated for this study are included in the manuscript and/or the Supplementary Files.

Declarations

Ethics approval and consent to participate

All applicable international, national, and/or institutional guidelines for the care and use of animals were followed.

Consent for publication

Not applicable.

Competing interests

The authors declare that the research was conducted in the absence of any commercial or financial relationships that could result in any potential conflict of interest.

Received: 30 August 2024 Accepted: 25 November 2024

Published online: 04 February 2025

References

- Acharya B, Chaijaroenkul W, Na-Bangchang K. Atractylodin inhibited the migration and induced autophagy in cholangiocarcinoma cells via PI3K/AKT/mTOR and p38MAPK signalling pathways. *J Pharm Pharmacol*. 2021;73:1191–200. <https://doi.org/10.1093/jpp/rgab036>.
- Acharya B, Chaijaroenkul W, Na-Bangchang K. Therapeutic potential and pharmacological activities of β -eudesmol. *Chem Biol Drug Des*. 2021;97:984–96. <https://doi.org/10.1111/cbdd.13823>.
- Chen C, Feng ZL, Petrović J, Soković M, Ye Y, Lin LG. Sesquiterpenoids from the sunflower family as potential anti-inflammatory candidates: a review. *Acta Materia Medica*. 2023;2:357–76. <https://doi.org/10.15212/AMM-2023-0026>
- Chen LG, Jan YS, Tsai PW, Norimoto H, Michihara S, Murayama C, Wang CC. Anti-inflammatory and Antinociceptive Constituents of *Atractylodes japonica* Koidzumi. *J Agric Food Chem*. 2016;64:2254–62. <https://doi.org/10.1021/acs.jafc.5b05841>.
- Qin J, Wang H, Zhuang D, Meng F, Zhang X, Huang H, Lv G. Structural characterization and immunoregulatory activity of two polysaccharides from the rhizomes of *Atractylodes lancea* (Thun.) DC. *Int J Biolog Macromole*. 2019;136:341–51. <https://doi.org/10.1016/j.ijbiomac.2019.06.088>.
- Xu R, Lu J, Wu J, Yu D, Chu S, Guan F, Liu W, Hu J, Peng H, Zha L. Comparative analysis in different organs and tissue-specific metabolite profiling of *Atractylodes lancea* from four regions by GC-MS and laser microdissection. *J Sep Sci*. 2022;45:1067–79. <https://doi.org/10.1002/jssc.202100924>.
- Zhang WJ, Zhao ZY, Chang LK, Cao Y, Wang S, Kang CZ, Wang HY, Zhou L, Huang LQ, Guo LP. *Atractylodis Rhizoma*: A review of its traditional uses, phytochemistry, pharmacology, toxicology and quality control. *Journal of Ethnopharmacology*. 2021;266: 113415. <https://doi.org/10.1016/j.jjep.2020.113415>.
- Zhang WJ, Bai QX, Cui GC, Zhang XJ, Lyu CG, Sun JH, Gao WY, Huang LQ, Guo LP. Recent progress and ongoing challenges in *Rhizoma atractylodis* research: biogeography, biosynthesis, quality formation and control. *MedPlant Biol*. 2023;2:19. <https://doi.org/10.48130/MPB-2023-0019>.

Publisher's Note

Springer Nature remains neutral with regard to jurisdictional claims in published maps and institutional affiliations.